Supplementary material for:

Carbon cycling on the East Siberian Arctic Shelf – a change in air-sea CO_2 flux induced by mineralization of terrestrial organic carbon

Erik Gustafsson[1, 2], Christoph Humborg[2, 3], Göran Björk[4], Christian Stranne[5, 6, 7], Leif G. Anderson[4], Marc C. Geibel[2, 3], Carl-Magnus Mörth[5, 6], Marcus Sundbom[3], Igor P. Semiletov[8, 9, 10], Brett F. Thornton[5, 6], Bo G. Gustafsson[1, 2]

[1]Baltic Nest Institute, Stockholm University, Stockholm, 10691, Sweden
[2]Baltic Sea Centre, Stockholm University, Stockholm, 10691, Sweden
[3]Department of Environmental Science and Analytical Chemistry, Stockholm University, Stockholm, 10691, Sweden
[4]Department of Marine Sciences, University of Gothenburg, Gothenburg, 40530, Sweden
[5]Department of Geological Sciences, Stockholm University, Stockholm, 10691, Sweden
[6]Bolin Centre for Climate Research, Stockholm University, Stockholm, 10691, Sweden
[7]Center for Coastal and Ocean Mapping, University of New Hampshire, Durham, 03824, New Hampshire, USA
[8]University of Alaska Fairbanks, International Arctic Research Center, Fairbanks, Alaska, 99775-7320, USA
[9]Tomsk Polytechnic University, Tomsk, 634050, Russia.
[10]Russian Academy of Sciences, Pacific Oceanological Institute, Vladivostok, 690041, Russia

Correspondence to: Erik Gustafsson (erik.gustafsson@su.se)

Contents

Table S1: Average annual runoff (km^3 y^{-1}) and average runoff in June (km^3) from the major rivers entering the Laptev and East Siberian Seas (data from R-ArcticNET; http://www.r-arcticnet.sr.unh.edu/v4.0/index.html).

Basin	River	Runoff (km^3 yr^{-1})	Runoff in June (km^3)
Laptev Sea	Khatanga	80	33
	Anabar	14	8.3
	Olenek	37	21
	Lena	490	160
	Yana	32	11
	Total	*650*	*234*
East Siberian Sea	Indigirka	50	15
	Alazeya	1.4	0.3
	Kolyma	100	39
	Bolshoy Anyuy	8.7	3.3
	Total	*160*	*57*

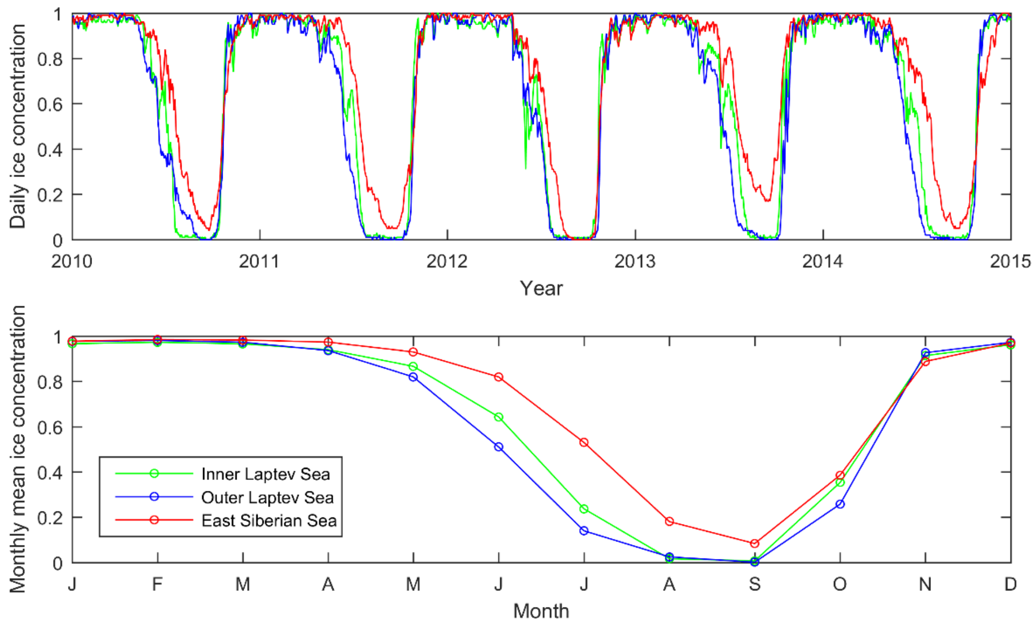

Figure S1: Observed daily ice concentrations (upper panel) and monthly mean ice concentrations in 2010-2014 (lower panel) in the three different sub-basins (data provided by the National Snow and Ice Data Centre; Cavalieri et al., 1996).

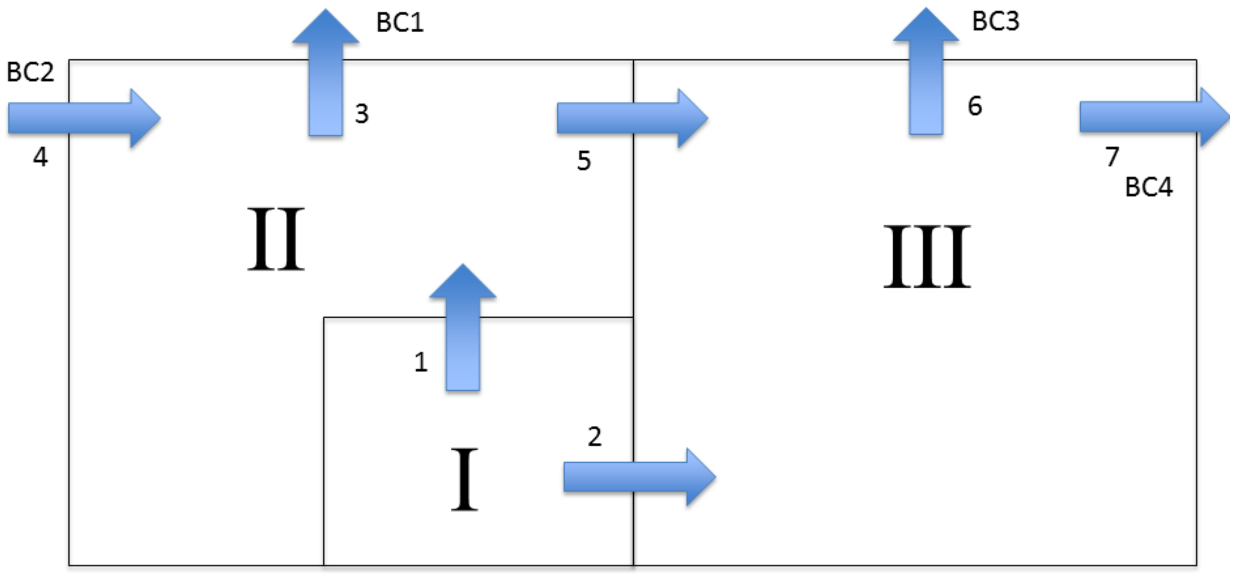

Figure S2: Basin layout, including the four model boundaries (BC1-4) and seven model straits.

S1. Atmospheric forcing

The relative humidity (RH) was obtained from the 2 m air temperature (T) and 2 m dew point temperature (T_{dp}) by calculating the ratio between actual vapor pressure (e_a) and saturation vapor pressure (e_s), and further utilizing the relation between actual vapor pressure and saturation vapor pressure at dew point temperature (i.e., $e_a(T) = e_s(T_{dp})$):

$$RH = 100\frac{e_s(T_{dp})}{e_s(T)} \quad (1)$$

The saturation vapor pressure was calculated as a function of temperature using the August-Roche-Magnus formula;

$$e_s(T) = c \cdot \exp\left(\frac{aT}{b+T}\right) \quad (2)$$

The saturation vapor pressure over water differs slightly from the corresponding value over ice, i.e., the constants a, b, and c are different in the two cases (Alduchov and Eskridge, 1996).

References

Alduchov, O. A., and Eskridge, R. E.: Improved Magnus Form Approximation of Saturation Vapor Pressure, J. Appl. Meteorol. Clim., 35(4), 601–609, doi:10.1175/1520-0450(1996)035<0601:IMFAOS>2.0.CO;2, 1996.

Cavalieri, D. J., Parkinson, C. L., Gloersen, P., and Zwally, H.: Sea Ice Concentrations From Nimbus-7 SMMR and DMSP SSM/I-SSMIS Passive Microwave Data (2010–2014), Natl. Snow and Ice Data Cent., Digital media, Boulder, Colo., doi:10.5067/8GQ8LZQVL0VL, 1996.